Journal of Nuclear Materials 448 (2014) 478–486

Contents lists available at ScienceDirect

Journal of Nuclear Materials

journal homepage: www.elsevier.com/locate/jnucmat

Effects of neutron irradiation on mechanical properties of silicon carbide composites fabricated by nano-infiltration and transient eutectic-phase process

Takaaki Koyanagi [a,*], Kazumi Ozawa [b], Tatsuya Hinoki [a], Kazuya Shimoda [a], Yutai Katoh [b]

[a] *Institute of Advanced Energy, Kyoto University, Gokasho, Uji, Kyoto 611-0011, Japan*
[b] *Materials Science and Technology Division, Oak Ridge National Laboratory, P.O. Box 2008, Oak Ridge, TN 37831, USA*

ARTICLE INFO

Article history:
Available online 10 October 2013

ABSTRACT

Unidirectional silicon carbide (SiC)-fiber-reinforced SiC matrix (SiC/SiC) composites fabricated by a nano-infiltration and transient eutectic-phase (NITE) process were irradiated with neutrons at 600 °C to 0.52 dpa, at 830 °C to 5.9 dpa, and at 1270 °C to 5.8 dpa. The in-plane and trans-thickness tensile and the inter-laminar shear properties were evaluated at ambient temperature. The mechanical characteristics, including the quasi-ductile behavior, the proportional limit stress, and the ultimate tensile strength, were retained subsequent to irradiation. Analysis of the stress–strain hysteresis loop indicated the increased fiber/matrix interface friction and the decreased residual stresses. The inter-laminar shear strength exhibited a significant decrease following irradiation.

Published by Elsevier B.V.

1. Introduction

The superior as-fabricated high-temperature mechanical properties and low-activation nuclear properties of silicon carbide (SiC)-fiber-reinforced SiC matrix (SiC/SiC) composites make them attractive as nuclear materials such as core constituents in light-water reactors, control rods for high-temperature gas-cooled reactors, and fusion blanket components [1]. Therefore, for nuclear applications, the mechanical performances of these materials must be retained under conditions of high temperature and neutron irradiation.

Among the industrially available SiC/SiC composites produced through various processing routes, chemically vapor-infiltrated (CVI) SiC matrix composites with the Generation III near-stoichiometric SiC fibers are presently considered as the reference nuclear grade materials. An extensive compilation of the neutron-irradiated properties for the CVI-SiC/SiC composites is now available [2]. Neutron-irradiated CVI-SiC/SiC composites, having less-crystalline SiC-based fibers and a highly crystalline matrix, reportedly exhibit interfacial debonding as a result of differential swelling between the fiber that densifies and swells under irradiation and the high-density matrix that only swells. Consequently, this results in degradation of the mechanical properties of the composite in the irradiated state [3]. In contrast, mechanical properties of the CVI-SiC/SiC composites that have highly crystalline fibers and matrices is not significantly altered subsequent to irradiation up to 40 dpa [4]. Thus, the combination of a highly crystalline fiber and matrix is essential for retention of mechanical properties during irradiation.

While CVI-SiC/SiC composites possess in general attractive properties, they are typified by 15–20% porosity. This translates into up to ~30% porosity in the matrix, considering the typical fiber volume fraction of ~35%, and is the major factor limiting the matrix cracking stress and thermal conductivity of these materials [2,5]. Moreover, it is relatively challenging for CVI-SiC/SiC composites to achieve gas tightness that is required for certain applications. The quest for SiC/SiC composites in which these limitations are circumvented by achieving dense matrices has led to the development of a nano-infiltration and transient eutectic-phase (NITE) process [6]. The NITE process applied to SiC/SiC composite production involves sintering of SiC nano-powder, carbon-coated highly crystalline SiC fibers, and oxide additives. The porosity achieved with this process is typically less than 5%, and excellent proportional limit stress (PLS), reaching up to ~360 MPa, has been reported for laboratory-grade NITE-SiC/SiC composites [7]. The thermal conductivities of NITE-SiC/SiC composites were also reportedly significantly higher than those of CVI-SiC/SiC composites in unirradiated conditions [8].

There is currently a dearth of available information about the effects of irradiation on the mechanical properties of NITE-SiC/SiC composites, and the radiation stability of SiC sintered with oxide additives is not well understood. The objective of this study is to determine the effects of neutron irradiation on the mechanical

* Corresponding author. Current address: Materials Science and Technology Division, Oak Ridge National Laboratory, 1 Bethel Valley Road, Oak Ridge, TN 37831-6140, USA. Tel.: +1 8655748764.

E-mail address: koyanagit@ornl.gov (T. Koyanagi).

0022-3115/$ - see front matter Published by Elsevier B.V.
http://dx.doi.org/10.1016/j.jnucmat.2013.10.005

properties of NITE-SiC/SiC composites. The irradiation strength of monolithic SiC, as the matrix material of the NITE-SiC/SiC composite, is also examined.

2. Experimental

Unidirectional Tyranno™-SA3 SiC fiber (product type: SA3-S1I16PX with nominal 7.5 μm diameter and 1600 filaments per yarn) reinforced NITE-SiC matrix composites (Pilot grade #3, Ube Industries, Ltd., Japan) were used as the test materials. Pyrolytic carbon (PyC) of 200–300 nm thickness was chemically vapor-deposited onto the fiber surfaces. The fiber volume fraction and porosity were ~45% and ~5%, respectively. Al_2O_3, Y_2O_3, and SiO_2 were used as sintering additives. Monolithic SiC, used as the matrix of the NITE-SiC/SiC composite, was fabricated; this material is referred to as NITE-SiC hereafter. The NITE-SiC was fabricated from β-SiC nano-powder (Sumitomo Osaka Cement Co. Ltd., Japan, T-1 grade), Al_2O_3 powder (Kojundo Chemical Laboratory Co. Ltd. Japan, mean diameter of 0.3 μm, 99.99% purity), Y_2O_3 powder (Kojundo Chemical Industries Ltd., Japan, mean diameter 1.0 μm, 99.99% purity), and SiO_2 powder (Kojundo Chemical Laboratory Co. Ltd., Japan, mean diameter of 1.0 μm, 99.9% up purity). The oxide additives, comprising a total of 12 wt%, were mixed with SiC powder and the combination was sintered by hot-pressing at 1800 °C, for 2 h, in an Ar atmosphere, under a pressure of 20 MPa. The porosity of NITE-SiC was less than 6%.

Neutron irradiation was conducted at the Japan Materials Testing Reactor (JMTR) located at the Oarai Research Establishment of the Japan Atomic Energy Agency or at the High-Flux Isotope Reactor (HFIR) located at Oak Ridge National Laboratory. The specimens were irradiated at 400–750 °C to 0.50–0.64 dpa for SiC (5.0–6.4 × 10^{24} n/m^2, E > 0.1 MeV; hereafter, 1.0 × 10^{25} n/m^2 = 1 dpa is assumed) for JMTR-04M18U campaign, at 600–800 °C to 0.52–0.77 dpa for JMTR-05M19U campaign, and at 830–1270 °C to 5.8–5.9 dpa for HFIR-RB*-18J campaign. The irradiation conditions are summarized in Table 1.

The tensile properties were examined using straight bar specimens, the dimensions of which were 40 mm (l) × 4 mm (w) × 2 mm (t). The fiber orientation was parallel to the loading direction. The tensile test was conducted in the cyclic loading mode. The peak tensile stress was incremented by 25 MPa in the repeated unloading–reloading sequences. The experimental procedure follows the general guidelines of ASTM C1275, with the exception that cyclic loading was adopted. PLS was defined as the stress at 5% stress deviation from the extrapolated linear segment used for the modulus determination. The trans-thickness tensile strength was evaluated using a diametral compression test method [9]. Truncated disk specimens (diameter: 4 mm, thickness: 5 mm, width: 3 mm) were used for this test. The interlaminar layer in the specimen was oriented parallel to the direction of compressive loading. The interlaminar shear strength was evaluated by the compression of double-notched specimens [10], according to ASTM C1292. Notched specimens were loaded parallel to the fiber longitudinal direction. For evaluation of the Weibull statistical strength of the NITE-SiC monolith, three-point flexural tests with a supporting span of 18 mm for the JMTR specimens and 1/4-four point flexural tests with an outer span of 20 mm NITE-SiC for the RB-*18J specimens were also conducted, as per ASTM C1161. The dimensions of the specimens were 24 or 25 mm (l) × 1 mm (w) × 1 mm (t). Dynamic Young's moduli of both the NITE-SiC/SiC composites and NITE-SiC were determined using the impulse excitation of vibration method in accordance with ASTM C1259. Microstructural observation of the unirradiated NITE-SiC and NITE-SiC/SiC composites was conducted using a field-emission scanning electron microscope (SEM, Ultra55, Zeiss). The post-irradiation experiments are summarized in Table 1. Three to six mechanical tests were performed under each condition (details of the valid test number are shown in Tables 2 and 3), except in the case of the flexural tests (16–30) for the Weibull statistical analysis. The results of mechanical tests on unirradiated NITE-SiC/SiC composites have been reported [11] and are updated in this study.

3. Results

Fig. 1 shows the secondary electron and backscattered electron images of the NITE-SiC/SiC composite and the backscattered electron image of monolithic NITE-SiC in the unirradiated condition. The NITE-SiC and the matrix of the NITE-SiC/SiC composite consist primarily of polycrystalline β-phase SiC and small amounts of oxide ceramics as the remnants of the sintering additives. The oxide grains in the NITE-SiC were found at the multi-grain junctions of the β-phase SiC grains and appeared to be homogeneously distributed with the monolithic body. In the case of the NITE-SiC/SiC composite, pores were observed in the fiber inter-bundles, and the oxide phases attributed to the sintering additives were observed both in the matrix-rich area and to have segregated to occupy the spaces within the fiber bundles and at the inter-bundle pockets.

The typical stress–strain curves from the cyclic unloading–reloading sequences are compared for the unirradiated and irradiated NITE-SiC/SiC composites in Fig. 2. The unirradiated composites exhibited quasi-ductile failure behavior, and such behavior was also observed after irradiation. Fig. 3 shows the maximum hysteresis loop width as a function of the matrix damage parameter [12]. The matrix crack spacing is theoretically inversely proportional to the matrix damage parameter (D) given by:

Table 1
Summary of neutron irradiation conditions and post-irradiation experiments for monolithic NITE-SiC and NITE-SiC/SiC composites. The checked marks denote tests conducted in the conditions studied.

Reactor	Capsule ID	T (°C)	ϕ (dpa)	Monolithic NITE-SiC			NITE-SiC/SiC composites			
				σ_{3pt}	σ_{4pt}	$E_{Dynamics}$	$E_{Dynamics}$	$\sigma_{Tensila}$	$\sigma_{Diameteral}$	σ_{DNS}
JMTR	04M-18U	400	0.50	√						
		600	0.55	√						
		750	0.64	√						
	05M-19U	600	0.52	√				√		
		800	0.77	√						
HFIR	RB*-18J	830	5.9		√	√	√	√	√	√
		1270	5.8		√	√	√	√	√	

T: irradiation temperature, ϕ: irradiation fluence, σ_{3pt}: three point flexural test, σ_{4pt}: 1/4-four point flexural test, $E_{dynamic}$: measurement of dynamic Young's modulus, $\sigma_{Tensile}$: tensile test, $\sigma_{Diametral}$: diametral compression test, σ_{DNS}: compression test using double notched specimen. It is noted that T (irradiation temperature) in the JMTR irradiations are nominal values, while the ones for the HFIR irradiation were determined by electrical resistivity change of isochronal annealing.

Table 2
Tensile properties of the non-irradiated and irradiated NITE-SiC/SiC composites. Average and ± one standard deviation are shown.

Irradiation condition	# of Valid tests	Tensile modulus (GPa)	Sonic modulus (GPa)	Proportional limit stress (MPa)	Ultimate tensile strength (MPa)	Strain at maximum load (%)
Unirradiated	5	343 ± 10	n/a	104 ± 25	399 ± 20	0.20 ± 0.03
600 °C 0.52 dpa	3	276 ± 10	n/a	127 ± 23	377 ± 19	0.20 ± 0.03
Unirradiated	6	274 ± 15	333 ± 5	142 ± 26	344 ± 25	0.17 ± 0.02
830 °C 5.9 dpa	5	289 ± 19	332 ± 8	152 ± 32	388 ± 32	0.18 ± 0.04
1270 °C 5.8 dpa	3	282 ± 8	345 ± 7	181 ± 46	404 ± 21	0.19 ± 0.01

# of Valid tests: number of valid tests, n/a: not available. Same shall apply to Tables 3–5.

Table 3
Effect of neutron irradiation on trans-thickness tensile strength of NITE-SiC/SiC composites. Average and ± one standard deviation are shown.

Irradiation condition	# of Valid tests	Trans thickness tensile strength (MPa)	Change by irradiation (%)
Unirradiated	4	21.4 ± 3.3	–
830 °C 5.9 dpa	6	18.9 ± 3.0	−11
1270 °C 5.8 dpa	4	26.4 ± 8.7	23

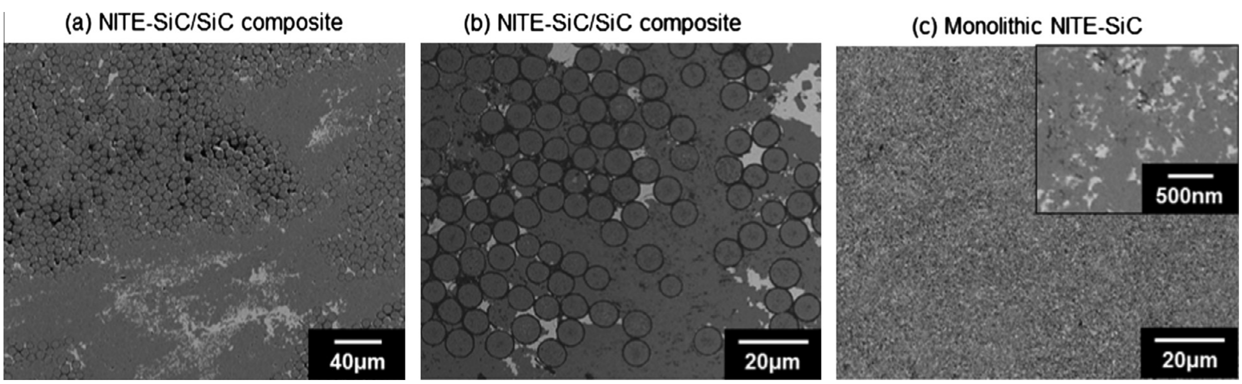

Fig. 1. SEM images for NITE-SiC/SiC composite and monolithic NITE-SiC: (a) secondary electron image, (b and c) backscattered electron image.

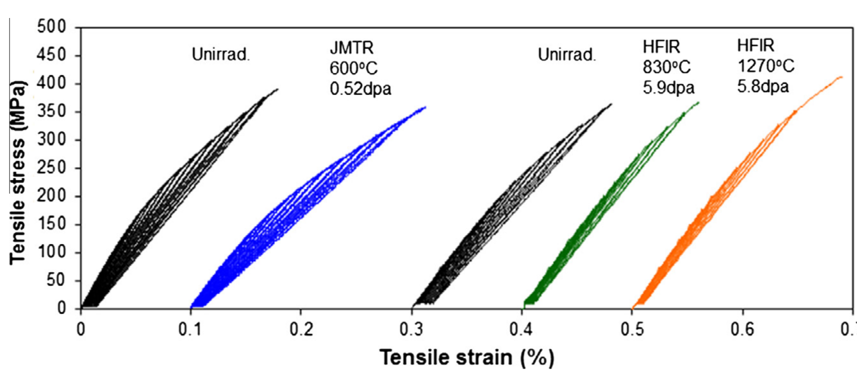

Fig. 2. Typical tensile stress–strain behaviors for the unirradiated and irradiated NITE-SiC/SiC composites. Each curve is offset horizontally for visibility.

$$D = \frac{E_c - E^*}{E^*} \quad (1)$$

where E_c and E^* are the modulus of the composite and the tangent modulus of the unloading curve, respectively, and D can be evaluated from each hysteresis loop [13]. It should be noted that the maximum hysteresis loop width was significantly reduced subsequent to irradiation. For instance, decreases in the unirradiated loop width by 58%, 89%, and 97% were observed at the matrix damage parameter of 0.15 following irradiation at the respective temperatures of 600, 830, and 1270 °C. Despite this significant change in the loop width, the irradiation effects on the mechanical properties were not significant. The tensile properties before and after irradiation are summarized in Table 2 and Fig. 4. The PLS remained unchanged, within the limits of statistical uncertainty, subsequent to irradiation. The effects of irradiation on Young's modulus were generally insignificant. The apparent Young's modulus decrease upon irradiation at 600 °C is due to the anomalously high modulus determined for the unirradiated specimen population as obvious in Table 2, likely caused by the spatial inhomogeneity of quality for this particular batch of material. The ultimate tensile strength (UTS) was statistically unchanged upon irradiation at 600 and 830 °C, but increased by 17% following irradiation at 1270 °C. The difference of modulus of the unirradiated materials between JMTR

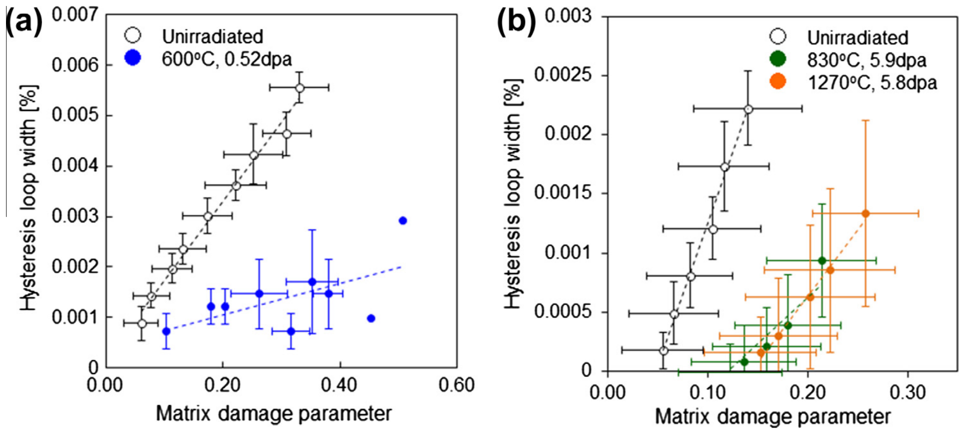

Fig. 3. The maximum hysteresis loop width as a function of matrix damage parameter before and after irradiation for the NITE-SiC/SiC composites: (a) irradiated at JMTR and (b) at HFIR.

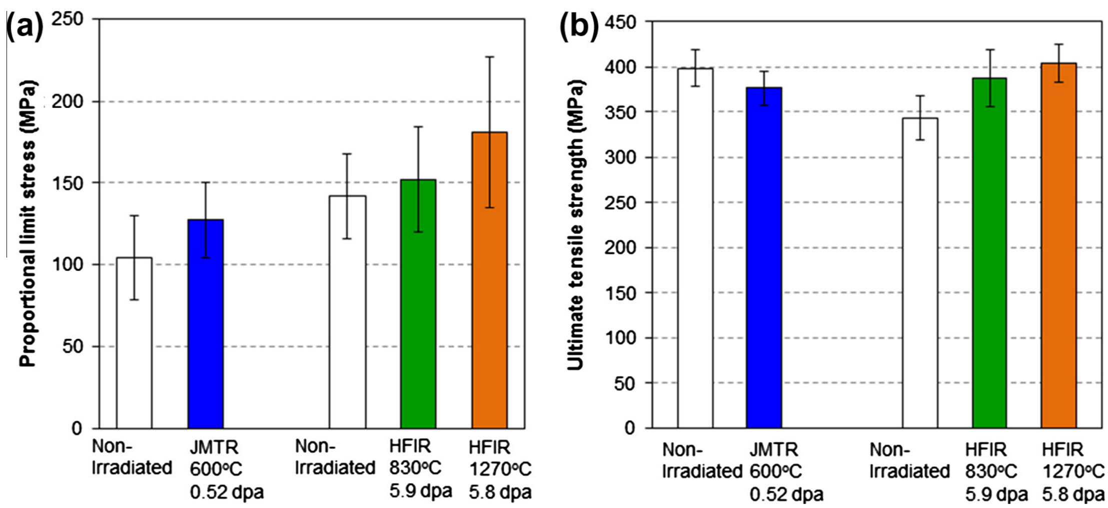

Fig. 4. Effects of neutron irradiation on (a) proportional limit stress and (b) ultimate tensile strength of NITE-SiC/SiC composites.

and HFIR irradiation was observed, which may come from a problem of the materials reproducibility.

Fig. 5 shows a typical stress–displacement curve of the diametral compression test and a typical optical micrograph for an unirradiated test specimen. All of the evaluated specimens failed by propagation of a crack along the loaded direction. Nozawa et al. reported that the initial fracture stress determined from the maximum fracture stress in the diametral compression test was

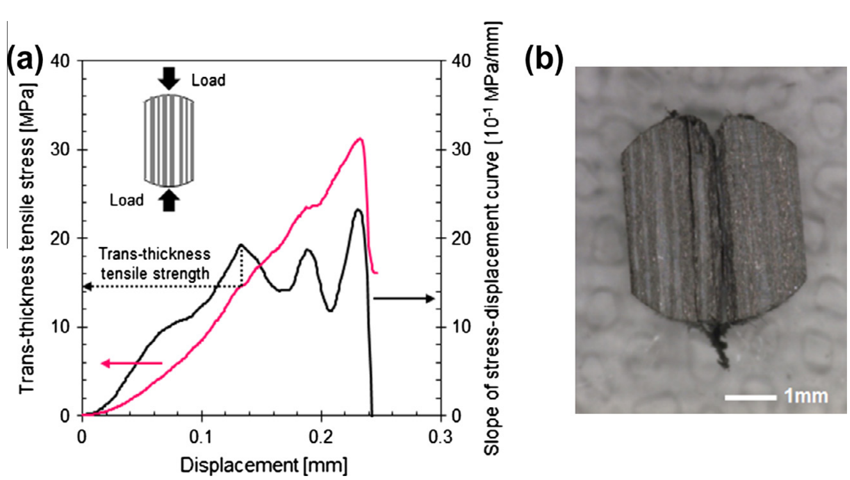

Fig. 5. (a) Typical fracture behavior of the NITE-SiC/SiC composite by the diametral compression test and (b) the typical image for the tested specimen in unirradiated condition.

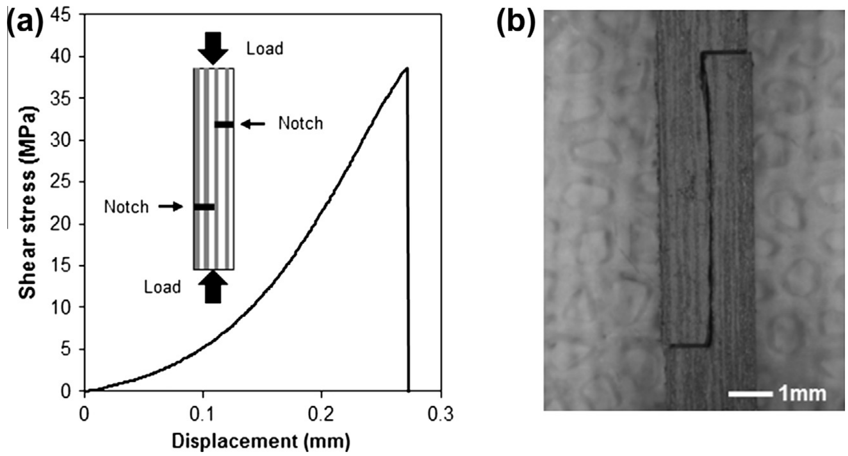

Fig. 6. (a) Typical fracture behavior of a double notched specimen of the NITE-SiC/SiC composite by the double notched shear test and (b) the typical image for the tested specimen in unirradiated condition.

Table 4
Interlaminar shear strength of the non-irradiated and irradiated NITE-SiC/SiC composites. Average and ± one standard deviation are shown.

Irradiation condition	# of Valid tests	Interlaminar shear strength (MPa)	Change by irradiation (%)
Unirradiated	4	37.2 ± 1.5	–
830 °C 5.9 dpa	3	25.4 ± 0.62	−31

Table 5
Summary of Weibull statistical analysis of the monolithic NITE-SiC evaluated by three or 1/4-four point flexure tests. The Weibull modulus and Weibull characteristic strength values are estimated by the maximum likelihood estimation. Range in the {} parenthesis indicates 95% confidence ration bounds for Weibull modulus.

Irradiation condition	# of Valid tests	Test method	Weibull modulus	Weibull characteristic strength (MPa)	Weibull mean strength (MPa)
Unirradiated	30	3 Point flexure	7.7 {4.9–8.3}	863 {814–918}	823
400 °C/0.50 dpa	16		4.1 {2.9–6.6}	704 {621–791}	644
600 °C/0.52 dpa	20		6.8 {4.1–8.0}	873 {808–954}	827
600 °C/0.55 dpa	20		6.1 {4.0–8.0}	716 {661–780}	675
750 °C/0.64 dpa	19		5.8 {3.9–7.8}	830 {760–906}	779
800 °C/0.77 dpa	20		6.2 {4.1–8.2}	951 {878–1033}	896
Unirradiated	30	1/4-4 Point flexure	6.3 {4.3–7.3}	634 {596–681}	598
830 °C/5.9 dpa	21		6.6 {3.9–7.3}	416 {384–456}	393
1270 °C/5.8 dpa	20		4.7 {3.3–6.6}	375 {338–414}	347

overestimated, and they found that execution of the diametral compression test using a pair of strain gauges or analysis using the slope of the stress–displacement curve facilitated more accurate determination of the initial fracture stress [14]. Herein, the analysis using the slope of the stress–displacement curves was adopted for unirradiated samples and those irradiated at 830 °C. The technique using the strain gauge was adopted for specimens irradiated at 1270 °C. The effects of irradiation on the trans-thickness tensile strength are summarized in Table 3. The trans-thickness tensile strength of 15 MPa for the unirradiated sample was not changed by irradiation at 830 and 1270 °C, considering the variability. However, the large variability obscures the irradiation effects on the trans-thickness tensile strength.

A typical stress–displacement curve of the compression test for the double-notched specimen and a typical image for an unirradiated test specimen are shown in Fig. 6. Interlaminar shear fractures appeared in the stress–displacement curve in the instant that the load reached its maximum, and notch to notch fractures were observed in all of the specimens. The interlaminar shear strength (25.4 MPa) for irradiation at 5.9 dpa at 830 °C was approximately 30% lower than that for the unirradiated sample (37.2 MPa), as shown in Table 4. Cracks had propagated through the matrix pores along the interface in unirradiated condition [11].

The Weibull statistical strength of monolithic NITE-SiC, evaluated on the basis of the flexure test, is summarized in Table 5. In addition, Fig. 7 shows the Weibull statistical three-point flexural strength at a relatively low temperature and fluence (~800 °C, ~0.77 dpa) for samples irradiated at JMTR, whereas Fig. 8 shows the 1/4-four point flexural strength at relatively high temperature and fluence (~830 °C, ~5.8 dpa) for samples irradiated at HFIR.

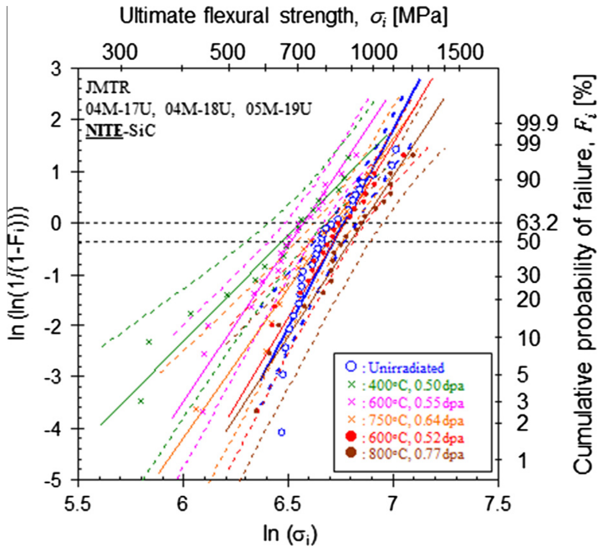

Fig. 7. Weibull statistical strength distribution of the monolithic NITE-SiC irradiated to relatively lower temperature and fluence (~800 °C, ~0.77 dpa), irradiated at JMTR. Dotted lines indicate 95% confidence bounds.

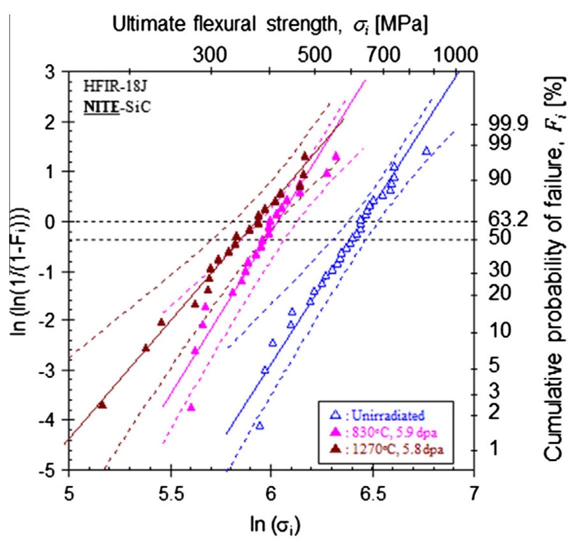

Fig. 8. Weibull statistical strength distribution of the monolithic NITE-SiC irradiated to relatively higher temperature and fluence (~830 °C, ~5.8 dpa), irradiated at HFIR. Dotted lines indicate 95% confidence bounds.

Significant degradation of the flexural strength as a result of irradiation was detected under the high temperature and dose conditions. For example, the Weibull characteristic strength was degraded by up to 18% upon irradiation to ~0.77 dpa. In comparison, the characteristic strength was degraded by respective values of 34% and 41% at 830 °C, 5.9 dpa and at 1270 °C, 5.8 dpa. The average dynamic Young's modulus of unirradiated NITE-SiC and the corresponding standard deviation were 344 and 7 GPa, respectively. The dynamic Young's modulus decreased by 5% following irradiation at 830 °C to 5.9 dpa, as well as at 1270 °C with irradiation to 5.8 dpa.

4. Discussion

4.1. Effects of irradiation on proportional limit stress

The PLS, which is an index of the matrix cracking stress, is in theory affected by the following parameters: (1) Young's moduli of the composite (E_c), fiber (E_f), and matrix (E_m); (2) the critical energy release rate for debonding at the fiber/matrix interface; (3) the critical mode-I matrix energy release rate; (4) the frictional stress at the fiber/matrix interface (τ); and (5) the thermal residual stress of the matrix in the tensile direction (σ_m) [15,16]. Thus, the PLS (σ_{PLS}) can be expressed as follows:

$$\sigma_{\rm PLS} = \sigma - \sigma_m \frac{E_c}{E_m} \tag{2}$$

where σ is a function of τ, E_f, E_m, the fiber volume fraction (V_f), the critical energy release rate for interfacial debonding, and the critical mode-I matrix energy release rate [15,16]. Based on Eq. (2), it is clear that the residual stress of the matrix in the tensile direction exerts a significant effect on the PLS. The other parameters are relatively ineffective to PLS in theory. The following paragraphs discuss the effects of irradiation on these parameters, which strongly influence the PLS of the NITE-SiC/SiC composite.

The effect of irradiation on Young's modulus of SiC has been studied using chemical vapor deposition (CVD) SiC as the matrix phase of the CVI-SiC/SiC composite. It is believed that Young's modulus of CVD-SiC declines slightly in response to irradiation-induced lattice expansion [17]. Previous work by Katoh et al. revealed that Young's modulus of CVI-SiC/SiC composites containing Tyranno™-SA3 fibers remained statically unchanged following irradiation to 5.9 dpa at 800 °C and to 5.8 dpa at 1300 °C [18]. This result indicates that Young's modulus of the Tyranno™-SA3 fibers also remained unchanged, considering the marginal decrease in the matrix modulus. Given that the irradiation conditions in Ref. [18] were similar to those used in this study, Young's modulus of the fibers in the NITE-SiC/SiC composites was expected to remain unchanged. On this basis, the insignificant effect of irradiation on Young's moduli of the NITE-SiC/SiC composites following irradiation both at 830 °C to 5.9 dpa and at 1270 °C to 5.8 dpa indicates that Young's modulus of the matrix was also maintained herein. In contrast, Young's modulus of the NITE-SiC/SiC composite decreased upon irradiation at 600 °C and 0.52 dpa, which may be attributed to dispersion of material quality, because modulus difference between uniradiated materials were observed as shown in Fig. 4. Degradation of the matrix modulus is also possible cause for this, given that a stable fiber modulus is expected, based on the insignificant degradation of Young's modulus of the CVI-SiC/SiC composite containing Tyranno™-SA3 fibers following irradiation at 610 °C and 1.9 dpa [19]. In summary, the effects of irradiation on Young's moduli of fiber and matrix were deemed to be insignificant in this study, except in the case of irradiation at 600 °C.

The effect of irradiation on the critical mode-I matrix energy release rate can be discussed using the strength and Young's modulus of monolithic NITE-SiC. If the effects of irradiation on the mechanical properties of monolithic NITE-SiC and the matrix of the NITE-SiC/SiC composite are similar, the critical matrix energy release rate should be decreased by irradiation at 830 and 1270 °C as a result of a significant reduction in the fracture strength (Table 4) and a minor reduction in the dynamic modulus of monolithic NITE-SiC. The effect of the decreased matrix energy release rate on the PLS is less certain, considering interfacial debonding at the fiber/matrix interface. In the case of very weak or strong interfacial debonding strength, the resulting decreased matrix energy release rate should contribute to the decreased PLS [15,16]. The mechanism of degradation of the strength of monolithic NITE-SiC is discussed below.

The thermal residual stress in the NITE-SiC/SiC composites is generated by mismatch of the coefficient of thermal expansion (CTE) of the fiber and the matrix during fabrication. The residual stress in the tensile direction can be estimated from the point of intersection of the average linear regression line of the respective unload–reload curves, as shown in Fig. 9 [20]. The stress level at the intersection point is referred to as the misfit stress. Fig. 10 shows the effect of irradiation on the misfit stress for the NITE-SiC/SiC composite. The positive misfit stress observed herein is indicative of the tensile residual stress in the matrix, and the error bars indicate the standard deviation. The unirradiated sample exhibited a misfit stress of 120 MPa, which decreased significantly to 35 MPa following irradiation at 600 °C. The initial value of 146 MPa of stress in the unirradiated sample also decreased to 94 and 83 MPa following irradiation at 830 and 1270 °C, respectively. The relationship between the misfit stress (σ_T) and the residual stress of the matrix in the tensile direction (σ_m) is given by [13]:

$$\sigma_m = \frac{E_m}{E_c}\sigma_T \tag{3}$$

From Eqs. (2) and (3), the PLS is directly affected by the misfit stress, and a reduction in the misfit stress should effectively contribute to increasing the PLS. Therefore, reduction of the misfit stress, i.e., reduction of the tensile residual stress of the matrix in the fiber axial direction, is one of the factors accounting for the maintained PLS subsequent to irradiation. It is postulated that the mechanisms underlying this modification of the residual stress include thermal and/or irradiation creep, secondary stress caused by the relatively higher degree of swelling of the matrix compared to the fiber [21], and the effect of irradiation on CTE.

The frictional stress at the fiber/matrix interface (τ) relates to the inelastic strain parameter (H), which can be estimated from the width of the maximum hysteresis loop [13]

$$H = \frac{b_2(1-a_1V_f)^2 R\sigma_p^2}{4d\tau E_m V_f^2} \tag{4}$$

Here, a_1 and b_2 are the Hutchinson and Jensen constants for Type II boundary conditions [22], V_f is the fiber volume fraction, R is the fiber radius, σ_p is the peak stress of the hysteresis loop, d is the matrix crack spacing, and E_m is Young's modulus of the matrix. The matrix crack spacing is theoretically inversely proportional to the matrix damage parameter (D) as shown in Eq. (1). Using the relationship between D and d, Eq. (4) can be rewritten as:

$$H = A\frac{D\sigma_p^2}{\tau} \tag{5}$$

where A is almost constant when Young's moduli of the fiber and matrix are stable under irradiation. The inelastic strain parameter (H) of the NITE-SiC/SiC composite is plotted against $D\sigma_p^2$, before and after irradiation in Fig. 9; the error bars show the standard deviations. Given that Young's moduli of the fiber and matrix were insensitive to irradiation at 830 and 1270 °C, as discussed above, the slope of the linear regression line should be inversely proportional to the interfacial frictional stress under these irradiation conditions. However, the frictional stress at 600 °C cannot be discussed, given that non-negligible degradation of the matrix modulus was indicated. Fig. 11 indicates approximately three- and 1.5-fold increases in the interfacial frictional stress following irradiation at 830 and 1270 °C, respectively, though there are large deviations possibly due to limited numbers of the tests. Theoretically, this increase should contribute to increasing the PLS [14,15]. Interfacial frictional stress is defined as the product of multiplication of friction coefficient and clamping stress. One possible mechanism for the increased frictional stress involves increased friction coefficient caused by grain growth in the fibers and matrix. Another possible mechanism is locally increased clamping stress and friction coefficient derived from the larger swelling of the oxide phases around the fibers compared to swelling of the fibers and matrix. Previous evaluation of the irradiation-induced swelling of a monolithic SiC indicated larger swelling of Y-Al oxide as a secondary phase in monolithic NITE-SiC [23]. The larger swelling of the oxide phases are also indicated by neutron irradiation experiment [24]. However, additional experimental data are required to clarify the mechanism

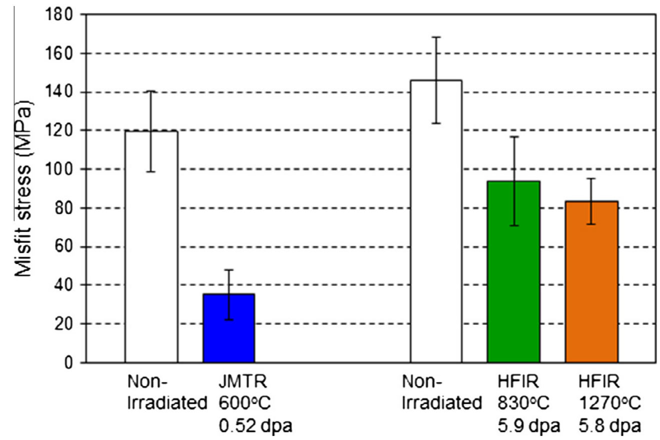

Fig. 10. Neutron irradiation effect on misfit stress in the NITE-SiC/SiC composites. It is noted that a positive sign denotes axial tensile residual stress in the matrix.

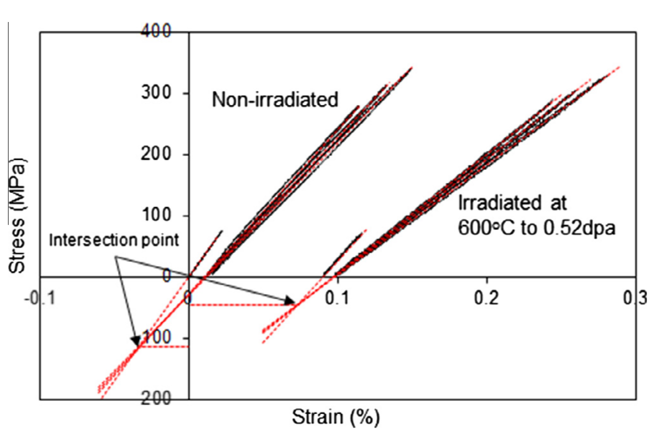

Fig. 9. One example of the determination method [17] for residual stress of tensile direction in matrix of the NITE-SiC/SiC composite.

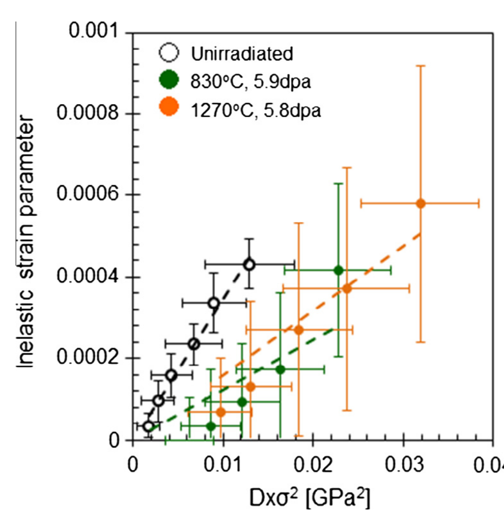

Fig. 11. Inelastic strain parameter as a function of matrix damage parameter multiplied by square of peak stress before and after irradiation for the NITE-SiC/SiC composites.

underlying the observed increase in the interfacial frictional stress caused by irradiation.

4.2. Effect of irradiation on the ultimate tensile strength

It is known that the UTS of unidirectional fiber-reinforced composites depends on the mechanical properties of the fiber and the interfacial frictional stress. When a matrix crack is ideally deflected at the fiber/matrix interface, the UTS (σ_u) is described by:

$$\sigma_u = f\sigma_0^{\frac{m}{m+1}}\left(\frac{\tau L_0}{R}\cdot\frac{2(m+1)}{(m+2)m}\right)^{1/(m+1)}\frac{m+1}{m+2} \tag{6}$$

where σ_0 is the Weibull mean strength, m is the Weibull modulus for the fiber strength, and L_0 is the gauge length [25]. The reported Weibull modulus for the strength of the Tyranno™-SA3 fiber was about 4 with and without irradiation to ~5.3 dpa at ~910 °C [18]. Thus, the fiber strength is a determining factor for the UTS. Katoh et al. demonstrated preservation of the UTS of a CVI-SiC/SiC composite containing Tyranno™-SA3 fibers subsequent to irradiation to 1.9 dpa at 610 °C, to 5.9 dpa at 800 °C, and to 5.8 dpa at 1300 °C, which are similar to the irradiation conditions used in this study [18,19]. This result implies the stability of the fiber strength under these irradiation conditions. Therefore, the excellent irradiation resistance of the UTS of the NITE-SiC/SiC composite is plausibly associated with the stable mechanical properties of the Tyranno™-SA3 fiber.

The UTS is also affected by the residual stress, given that the residual stress in the fiber radial direction affects the bonding strength at the fiber/matrix interface, with a consequent effect on the deflection of the matrix crack at the interface. The hysteresis loop analysis shown in Fig. 10 revealed the existence of tensile residual stress of the matrix in the fiber axial direction. This result is consistent with a larger CTE of the matrix relative to the fiber and the existence of compressive stress at the fiber/matrix interface in the fiber radial direction, based on the fiber–matrix concentric two-cylinder model [15]. Considering the decreased misfit stress following irradiation, it is expected that the residual compressive stress in the fiber radial direction was decreased as a result of irradiation. This decrease in the compressive stress should decrease the strength of interfacial bonding and consequently promote the deflection of the matrix crack, which should contribute to increasing the UTS. Therefore, the 17% increase in the UTS at 1270 °C may be explained in terms of a decrease in the strength of the interfacial debonding as a result of modification of the residual stress.

4.3. Effect of irradiation on the mechanical properties of NITE-SiC

The flexural strength of NITE-SiC was significantly degraded by irradiation in this study, which agrees with previous research on the effects of the irradiation strength on SiC containing a secondary phases [17]. As discussed above, the microstructure of NITE-SiC consists primarily of β-phase SiC with small amount of oxide ceramics. Since β-phase SiC in a high purity polycrystalline form is reportedly very stable in the irradiation conditions of this study [17], the observed detrimental effect of irradiation on strength of NITE-SiC is attributed to the presence of the oxide secondary phases.

One known mechanism that explains the irradiation-induced strength deterioration for SiC with secondary phases involves micro-cracking caused by the misfit stress due to the differential swelling between the secondary phase and SiC. However, in the present case, an extensive micro-crack generation is unlikely given that only ~5% decrease in Young's modulus was observed following irradiation at 830 and 1270 °C. However, the misfit stress caused by differential swelling is a plausible cause of the degradation of the flexural strength as a result of irradiation. Other possible reasons include the strength degradation of the secondary phase itself and degradation of the grain boundary strength due to the likely presence of oxide films at the SiC grain boundaries.

It is interesting to note that the PLS of NITE-SiC/SiC composite did not exhibit any irradiation-induced degradation that is inconsistent with the strength decrease for NITE-SiC, because the matrix material of NITE-SiC/SiC composite is similar with the monolithic NITE-SiC. This may be caused by the contribution of residual stress change to the PLS as discussed in Section 4.1. Additional possible explanation for this discrepancy is the effect of oxide segregation into the fiber-rich regions within NITE-SiC/SiC composite, resulting in the decreased oxide contents in the matrix-rich volume. In this way, the misfit stress due to the excess swelling of the oxide phases may be better withstood by the presence of adjacent or nearby fibers that are much stronger than the matrix. However, additional microscopical and microchemical analyses of the fracture surfaces will be necessary to determine the exact reason for the observed strength degradation of NITE-SiC.

4.4. Effect of irradiation on trans-thickness tensile and interlaminar shear strengths

Based on the SEM image presented in Fig. 1, pores in the fiber bundle are the most probable origin of the fracture in the diametral compression test. Cracks originating at the fiber bundle plausibly propagated to the matrix-rich region surrounding the fiber bundle, with subsequent fracture of the matrix at the trans-thickness tensile strength region. Based on this consideration, the trans-thickness tensile strength should be closely-related to the fracture toughness of the matrix. Herein, the effects of irradiation on the trans-thickness tensile strength were insignificant at 830 and 1270 °C. Therefore, this result implies that there is no significant degradation of the fracture toughness of the matrix.

Nozawa et al. demonstrated that the trans-thickness tensile strength of a unidirectional NITE-SiC/SiC composite was similar to its 90° off-fiber-axial tensile strength [14]. They also demonstrated that the combination of the 90° off-axial tensile strength, interlaminar shear strength, and axial tensile strength was useful for predicting the anisotropy of the strength (e.g., off-fiber-axial tensile strength) of the NITE-SiC/SiC composite [14]. In this study, no significant degradation of the 90° off-axial tensile strength was indicated by the diametral compression test following irradiation at 830 and 1270 °C. Moreover, the axial tensile strength was not degraded under the afore-stated irradiation conditions. In contrast, the interlaminar shear strength evaluated using the double-notched specimen decreased by 30% following irradiation at 830 °C. These results imply that the anisotropy of the strength of the unidirectional NITE-SiC/SiC composite at 830 °C may be modified by the degradation of the interlaminar shear strength. The interfacial shear strength should relate to the shear strength at the fiber/matrix interface because cracks appeared to propagate the interface in fracture surface of the double-notched specimens. Therefore, the degradation of interfacial shear strength can be understood by the degradation of the strength of the PyC interface.

5. Conclusions

No significant effects of neutron irradiation on the tensile properties such as quasi-ductile behavior, PLS, and UTS of the unidirectional Tyranno™-SA3 fiber-reinforced NITE-SiC/SiC composites were observed subsequent to irradiation with 0.52 dpa at 600 °C, with 5.9 dpa at 830 °C, and with 5.8 dpa at 1270 °C. In contrast, hysteresis loop analysis indicates an increase in the frictional stress at the fiber/matrix interface at 830 and 1270 °C, which is possibly caused by the locally increased clamping stress and friction coefficient derived from the larger swelling of the secondary phase compared to swelling of the fibers and matrix. Hysteresis loop analysis also further indicated reduction of the tensile residual stress of the matrix in the fiber axial direction for all of the irradiation conditions considered.

Significant degradation of the flexural strength of monolithic NITE-SiC, which represented as the matrix of the NITE-SiC/SiC composite, was demonstrated following irradiation at 830 and 1270 °C, whereas the PLS of the NITE-SiC/SiC composites did not exhibit any degradation. Effectively contribution to increasing the PLS was theoretically brought form residual stress modification of the matrix as described above, which accounts in part for the excellent irradiation resistance of the PLS.

The excellent irradiation resistance of the ultimate tensile strength was plausibly attributed to the stable mechanical properties of the Tyranno™-SA3 fiber following irradiation.

The interlaminar shear strength of NITE-SiC/SiC composites was decreased by 30% subsequent to irradiation at 830 °C. This can be understood by the degradation of the strength of the PyC interface.

Acknowledgements

This work was supported by Office of Fusion Energy Sciences under contract DE-C05-00OR22725 with UT-Battelle, LLC, and US-Japan TITAN Collaboration on Fusion Blanket Technology and Materials. Research was supported in part by High Flux Isotope Reactor, which is sponsored by the Office of Basic Energy Sciences, U.S. Department of Energy, and International Research Center for Nuclear Materials Science, Institute for Materials Research, Tohoku University. The first author was partly supported by a Grant-in-Aid for JSPS Fellows 24-3915.

The authors thank L.T. Gibson, A.M. Williams, P.S. Tedder, A.D. Harrison, S.G. Beck, L.E. Reid, and B.D. Johnson for post-irradiation experiments in ORNL and M. Narui, H. Kishimoto, S. Kondo, Y.-B. Choi, M. Yamasaki, S. Terunuma, T. Terunuma, Y. Maki, S. Ikeda, K. Toyoshima, and Y. Kawashima, and M.-K. Kim for assistance with post-irradiation experiments at Tohoku University.

References

[1] Y. Katoh, L.L. Snead, I. Szlufarska, W.J. Weber, Curr. Opin. Solid State Mater. Sci. 16 (2012) 143–152.
[2] Y. Katoh, K. Ozawa, C. Shih, T. Nozawa, R.J. Shinavski, A. Hasegawa, L.L. Snead, J. Nucl. Mater. 448 (2014) 448–476. <http://dx.doi.org/10.1016/j.jnucmat.2013.06.040>.
[3] L.L. Snead, D. Steiner, S.J. Zinkle, J. Nucl. Mater. 191–194 (1992) 566–570.
[4] Y. Katoh, T. Nozawa, L.L. Snead, K. Ozawa, H. Tanigawa, J. Nucl. Mater. 417 (2011) 400–405.
[5] J.A. DiCarlo, H.-M. Yun, G.N. Morscher, R.T. Bhatt, SiC/SiC composites for 1200 °C and above, in: N.P. Bansal (Ed.), Handbook of Ceramic Composites, Springer Science + Business Media Inc., New Yotk, 2005, pp. 77–98.
[6] Y. Katoh, S.M. Dong, A. Kohyama, Fusion Eng. Des. 61–62 (2002) 723–731.
[7] K. Shimoda, A. Kohyama, T. Hinoki, Compos. Sci. Technol. 69 (2009) 1623–1628.
[8] K. Shimoda, J.S. Park, T. Hinoki, A. Kohyama, J. Nucl. Mater. 386–388 (2009) 634–638.
[9] T. Hinoki, E. Lara-Curzio, L.L. Snead, Ceram. Eng. Sci. Proc. 24 (2003) 401.
[10] E. Lara-Curzio, D. Bowers, M.K. Ferber, J. Nucl. Mater. 230 (1996) 226–232.
[11] Y.B. Choi, T. Hinoki, K. Ozawa, Y. Katoh, K. Matsugi, T. Kelimu, Mater. Trans. 53 (2012) 2060–2063.
[12] M.Y. He, B.-X. Wu, A.G. Evans, J.W. Hutchinson, Mech. Mater. 18 (1994) 213–229.
[13] E. Vagaggini, J.M. Domergue, A.G. Evans, J. Am. Ceram. Soc. 78 (1995) 2709–2720.
[14] T. Nozawa, K. Ozawa, Y.B. Choi, A. Kohyama, H. Tanigawa, Fusion Eng. Des. 87 (2012) 803–807.
[15] B. Budiansky, J.W. Hutchinson, A.G. Evans, J. Mech. Phys. Solids 34 (1986) 167–189.
[16] M. Sutcu, W.B. Hillig, Acta Metall. Mater. 38 (1990) 2653–2662.
[17] L.L. Snead, T. Nozawa, Y. Katoh, T.S. Byun, S. Kondo, D.A. Petti, J. Nucl. Mater. 371 (2007) 329–377.
[18] Y. Katoh, K. Ozawa, T. Hinoki, Y. Choi, L.L. Snead, A. Hasegawa, J. Nucl. Mater. 417 (2011) 416–420.
[19] Y. Katoh, L.L. Snead, T. Nozawa, S. Kondo, J.T. Busby, J. Nucl. Mater. 403 (2010) 48–61.
[20] M. Steen, J.L. Valles, Unloading–reloading sequence and the analysis of mechanical test results for constituents fiber ceramic composites, in: M.G. Jenkins, E. Lara-Curizo, S.T. Gonczy, N.E. Ashbaugh, L.P. Zawada (Eds.), Thermal and Mechanical Test Method and Behavior of Continuous Fiber Ceramic Composites ASTM STP 1309, ASTM, West Conshohocken, 1996, pp. 49–65.
[21] T. Koyanagi, S. Kondo, T. Hinoki, J. Nucl. Mater. 442 (2013) S380–S383.
[22] J.W. Hutchinson, H.M. Jensen, Mech. Mater. 9 (1990) 139–163.
[23] T. Koyanagi, S. Kondo, T. Hinoki, J. Nucl. Mater. 417 (2011) 435–439.
[24] Ozawa K, Katoh Y, Snead LL, Nozawa T, Hinoki T, Hasegawa A. Fusion Materials Semiannual Progress, Report DOE/ER-0313/46, 2009, pp. 4–15.
[25] W.A. Curtin, B.K. Ahn, N. Takeda, Acta Mater. 46 (10) (1998) 3409–3420.